Dissolved organic matter and inorganic mercury loadings increase methylmercury production,

Clostridia abundance, and recalcitrant organic matter processing in oligotrophic sediments

Emily B. Graham[1*], Joseph E. Knelman[2], Rachel S. Gabor[3], Shon Schooler[4], Diane M. McKnight[5,6,7], Diana R. Nemergut[5,8]

[1]Biological Sciences Division, Pacific Northwest National Laboratory, Richland, WA, USA

[2]Joint Genome Institute, US Department of Energy, Walnut Creek, CA, USA

[3]Department of Geology and Geophysics, University of Utah, Salt Lake City, UT, USA

[4]Lake Superior National Estuarine Research Reserve, University of Wisconsin-Superior, Superior, WI, USA

[5]Institute for Arctic and Alpine Research, University of Colorado at Boulder, Boulder, CO, USA

[6]Civil Engineering Department, University of Colorado at Boulder, Boulder, CO, USA

[7]Environmental Studies Program, University of Colorado at Boulder, Boulder, CO, USA

[8]Biology Department, Duke University, Durham, NC, USA

Correspondence:

Emily B. Graham, emily.graham@colorado.edu

Biological Sciences Division, Pacific Northwest National Laboratory

902 Battelle Blvd.

Richland, WA, 99354, (509) 372-6049

1   **Abstract.**

2   Advances in genetics have allowed for greater investigation into the complex microbial

3   communities mediating mercury methylation in the environment. In wetlands in particular,

4   dissolved organic matter (DOM) may influence methylmercury production both through direct

5   chemical interactions with mercury and through substrate effects on the environmental

6   microbiome. We conducted microcosm experiments in two chemically disparate wetland

7   environments (unvegetated and vegetated sediments) to examine the impact of DOM from

8   leachate of local vegetation and inorganic mercury loadings on microbial community

9   membership, metagenomic potential, DOM processing, and methylmercury (MeHg) production.

10   We show that while DOM loadings impacted the microbiome in both environment types,

11   sediment with high organic carbon content was more resistant than oligotrophic sediment to

12   changes in microbiomes. Oligotrophic sediments receiving DOM produced significantly more

13   MeHg than unamended microcosms, coincident with an increase in putative chemoorganotrophic

14   methylators within the class *Clostridia*. Further, metagenomic shifts toward fermentation, and

15   secondarily iron metabolisms, in these microcosms as well as degradation of complex DOM

16   indicated by fluorescence indices also support a possible association between rarely

17   acknowledged microbial metabolisms and MeHg production. Our research provides a basis for

18   future investigation into the role of fermenting organisms in mercury toxicity and generates a

19   new hypothesis that DOM can stimulate mercury methylation in oligotrophic environments

20   either 1) via direct methylation by fermenting bacteria or 2) via enhancing the bioavailability of

21   simple carbon compounds for sulfate- and iron-reducing bacteria through breakdown of complex

22   DOM.

23   **Introduction.**

24   Mercury methylation in anoxic sediments is central to the bioaccumulation of mercury in

25   plant and animal tissue (Benoit *et al.* 2003, Morel *et al.* 1998, Ullrich *et al.* 2001) and poses a

26   significant environmental and human health concern in freshwater wetlands (Branfireun *et al.*

27   1999, Harmon *et al.* 2005, Jeremiason *et al.* 2006). Dissolved organic matter (DOM) has been a

28   focus of geochemical investigations for decades, and both positive and negative interactions

29   between DOM and mercury methylation – principally, a microbial transformation (reviewed in

30   Hsu-Kim *et al.* 2013) – have been demonstrated under contrasting environmental conditions

31   (Graham *et al.* 2013, Hsu-Kim *et al.* 2013, Ravichandran 2004). While the microbial

32   mechanisms generating methylmercury are poorly understood, the recent discovery of the *hgcAB*

33   gene cluster has allowed investigations into the microbial ecology of mercury cycling (Gilmour

34   *et al.* 2013, Parks *et al.* 2013, Poulain and Barkay 2013, Smith *et al.* 2015). In particular,

35   interactions between environmental microbiomes, DOM quantity and quality, and mercury

36   methylation in natural systems remain an uncertainty in predicting hotspots of mercury toxicity

37   in the environment (reviewed in Hsu-Kim *et al.* 2013, Podar *et al.* 2015).

38   Dissolved organic matter is comprised of various classes of organic compounds

39   (primarily organic acids) with a wide range of molecular weights and aromaticities (Lambertsson

40   and Nilsson 2006, Wetzel 1992). DOM concentrations are elevated in wetlands relative to other

41   freshwater systems (>10 mg/L), and the humic fraction derived from plant leachate

42   predominates. With respect to mercury cycling in wetlands, mercury methylation is impacted

43   both by binding properties of the humic DOM fraction, resulting either in increased dissolution

44   of inorganic mercury complexes or in physical inhibition of mercury bioavailability (Drexel *et*

45   *al.* 2002, Haitzer *et al.* 2002, Waples *et al.* 2005), and by provisioning organic substrate for

46   microbial activity (Hsu-Kim *et al.* 2013, King *et al.* 2000, Lambertsson and Nilsson 2006).

47   These effects may also vary with ambient geochemistry, as Graham *et al.* (2013) have

48   demonstrated that sulfide concentrations and DOM aromaticity interact to influence MeHg

49   production. Further, interactive effects of sediment microbiomes and DOM biogeochemistry are

50   less well-resolved than other aspects of linkages between environmental geochemistry and

51   mercury toxicity. Numerous studies have shown regulation of freshwater microbial communities

52   by DOM quantity or quality (Docherty *et al.* 2006, Forsström *et al.* 2013, Pernthaler 2013), and

53   such changes in environmental microbiomes may alter ecosystem biogeochemical cycling

54   (Graham *et al.* 2016). The character of humic DOM thought to be most influential to mercury

55   methylation can be assessed at scales relevant to microbial activity with fluorescence

56   spectroscopy, which correlates changes in humic fluorescence relative to other portions of the

57   optically-active DOM pool (Fellman *et al.* 2010).

58   Recent work has increased knowledge on the microbiology of mercury methylation,

59   expanding potential microorganisms mediating methylation beyond sulfate-reducing bacteria

60   (Compeau and Bartha 1985, reviewed in Hsu-Kim *et al.* 2013), iron-reducing bacteria (Kerin *et*

61   *al.* 2006) and methanogens (Hamelin *et al.* 2011). To date, all tested microorganisms containing

62   the *hgcAB* gene cluster have been confirmed as methylators (Gilmour *et al.* 2013, Hsu-Kim *et al.*

63   2013). Gilmour *et al.* (2013) have identified five clades of putative methylators, including new

64   clades of syntrophic and *Clostridial* organisms. While research has provided insight into the

65   abundance of these new organisms in mercury-contaminated landscapes (Bae *et al.* 2014,

66   Hamelin *et al.* 2015, Liu *et al.* 2014a), many studies have continued to focus on the involvement

67   of sulfate- (Liu *et al.* 2014b, Lu *et al.* 2016) and iron-reducing bacteria (Si *et al.* 2015) as well as

68   methanogens (Yu *et al.* 2013) in mercury methylation. As such, the importance of organisms

69   with alternative metabolisms in mercury methylation remain relatively unexplored. Resolving

70   interactions between sediment microbiomes, environmental chemistry, and inorganic mercury

71   complexes is thought to be central in understanding variation in methylation rates among natural

72   systems (Gilmour *et al.* 2013, Hintelmann *et al.* 2000, Hsu-Kim *et al.* 2013).

73   Here, we examine the influence of plant leachate and inorganic mercury loadings on net

74   methylmercury (MeHg) production in a contaminated freshwater estuary at the base of Lake

75   Superior. We hypothesize that environmental biogeochemistry (in particular, DOM quantity and

76   quality) influences mercury methylation both by regulating microbial activity and by shifting the

77   abundance and metabolic diversity of mercury methylators. We test this hypothesis across

78   chemically distinct oligotrophic versus high carbon (C) sediments associated with unvegetated

79   and vegetated environments, using a microcosm experiment to monitor changes in sediment

80   microbiomes, DOM chemical quality, and net MeHg production in response to additions of

81   leachate from overlying plant material and inorganic mercury. Our results provide evidence for

82   the involvement of metabolisms that ferment recalcitrant organic matter in mercury methylation,

83   particularly within oligotrophic environments, an effect that may be imperative to understanding

84   and mitigating human exposure to MeHg with increasing rates of anthropogenic eutrophication.

85   **Methods.**

86   *Field site.*

87   The St. Louis River Estuary is home to the largest U.S. port on the Great Lakes and

88   covers roughly 12,000 acres of wetland habitat directly emptying into Lake Superior. Mining in

89   the headwaters, industrial discharge in the port, and atmospheric deposition have left a legacy of

90   mercury contamination in the sediment. We obtained sediment samples from wild rice

91   (*Zizania palustris*, 46° 40.855' N, 91° 59.048'W) and unvegetated (46° 41.918' N, 92° 0.123' W)

92   patches in Allouez Bay, which has high mercury concentrations relative to other areas of the

93   estuary (data not shown). We also obtained wild rice plant matter from nearby Pokegama Bay

94   (46.683448°N, 92.159261°W). Both habitats are clay influenced embayments that drain an

95   alluvial clay plain created by deposition during the retreat of the last glaciation approximately

96   10,000 years BP.

97   *Experimental design.*

98   A total of 20 anoxic microcosms were constructed in September 2013 to investigate

99   relationships between sediment microbiomes, DOM chemical quality, and mercury methylation.

100   Sediment was obtained in 250-mL amber Nalgene bottles from the top 10 cm of sediment using a

101   block sampling design described in the Supplemental Material. Leachate was extracted using 1 g

102   dried, ground plant matter:20 mL of Nanopure water, filtered through Whatman 0.7 μm GFF

103   filters (Whatman Incorporated, Florham Park, NJ, USA). Microcosms were constructed in 500-

104   mL airtight glass mason jars and stored at room temperature in the dark in Mylar bags with

105   oxygen-absorbing packets between subsampling. Our experiment was designed to promote

106   microbial MeHg production by minimizing abiotic photo-methylation and -demethylation (Morel

107   *et al.* 1998) and sustaining a low redox environment to inhibit demethylation (Compeau and

108   Bartha 1984). A full-factorial design was employed with two environments (vegetated and

109   unvegetated sediment) and two treatments (plant leachate and Nanopure water). Each microcosm

110   received 100 g wet sediment, and 250 mL solution consisting either of DOM at 100 mg/L and

111   $HgCl_2$ at 20 mg/L (50 μg/g wet sediment) in Nanopure water (DOM-amended replicates) or

112   solely of $HgCl_2$ at 20 mg/L in nanopure water (controls). Addition of $HgCl_2$ at high concentration

113   negated initial differences in mercury and provided substrate for the duration of the experiment.

114   $HgCl_2$ concentrations were comparable to microcosm experiments of similar design (Harris-

115   Hellal *et al.* 2009, Poulain *et al.* 2006, Ruggiero *et al.* 2011, Zhou *et al.* 2012). Microcosms were

116   incubated for 28 days, and subsamples of sediment and water were taken every seven days for

117   analysis of sediment microbiomes and DOM characteristics. All sample processing was

118   conducted in an anaerobic glovebox containing 85% N_2, 5% CO_2, and 10% H_2 gas mix at the

119   USGS in Boulder, CO.

120   *Sediment chemistry, extracellular enzyme activity, and mercury methylation.*

121   Percent carbon and nitrogen, NO_3^-/NO_2^-, NH_4^+, total particulate organic carbon (TPOC),

122   total dissolved nitrogen (TDN), pH, and extracellular enzyme activities of β-1,4-glucosidase, β -

123   1,4-N-acetylglucosaminidase, and acid phosphatase were determined on pre-incubation

124   sediments, as described in the Supplemental Material. For total- and methylmercury analysis,

125   initial (T0) and final (T4) subsamples were frozen at -70^oC, freeze-dried, and sent on dry ice to

126   the USGS Mercury Lab in Middleton, WI for analysis by aqueous phase ethylation, followed by

127   gas chromatographic separation with cold vapor atomic fluorescence detection (Method 5A-8)

128   and acid digestion (Method 5A-7). Mercury analyses were performed on 3 of 5 replicates for

129   each environment and microcosm type. All other analyses were performed on 5 replicates,

130   except for unvegetated controls beyond T0 ($n = 4$, one replicate destroyed during experiment).

131   *Dissolved organic matter characteristics.*

132   Water subsamples were collected at 7-day intervals (T0, T1, T2, T3, T4) to determine

133   non-purgeable organic carbon (NPOC) concentration and specific UV absorbance at 254 nm

134   ($SUVA_{254}$) as well characteristics of the optically active DOM pool (mostly associated with

135   humic DOM fraction), as described in the Supplemental Material. We calculated the

136   fluorescence index (FI) to determine the relative contribution of microbial vs. terrestrial matter to

137   the DOM pool, the humic index (HIX) to identify large aromatic compounds consistent with

138   humic material, and the freshness index to determine the availability of labile carbon (reviewed

139   in Fellman *et al.* 2010, Gabor *et al.* 2014a) using MATLAB software (2013a, The MathWorks,

140   Natick, MA) according to Gabor *et al.* (2014b).

141   *Microbial DNA extraction, 16S rRNA amplicon, and metagenomic shotgun sequencing.*

142   DNA from each sediment subsample was extracted using the MO Bio Power Soil DNA

143   Extraction kit (MO BIO Laboratories, Carlsbad, CA, USA), as described in Knelman *et al.*

144   (2012). The region encoding the V4 fragment of the 16S rRNA gene was amplified with the

145   primers 515F/806R, using the PCR protocol described by the Earth Microbiome Project

146   (Supplemental Material, Caporaso *et al.* 2012). The final multiplexed DNA samples were

147   sequenced at CU-Boulder (BioFrontiers Institute, Boulder, CO) on an Illumina MiSeq with the

148   MiSeq Reagent Kit v2, 300 cycles (Illumina, Cat. # MS-102-2002) to generate 2 x 150-bp

149   paired-end reads. Sequences are available at XXXXXX. In addition, 3 unvegetated DOM-

150   amended replicates at T0 (before leachate additon) and T4 were sent to the Joint Genome

151   Institute (JGI) for shotgun metagenomic sequencing on the Illumina HiSeq platform. Sequences

152   are available at XXXXX.

153   *Sequence analysis.*

154   Partial 16S rRNA gene were filtered for sequence length and minimum quality score in

155   the UPARSE pipeline (Edgar 2013) and OTUs were assigned using QIIME (Supplemental

156   Material, Caporaso *et al.* 2010). Metagenomic shotgun sequences were assembled and classified

157   against the protein families database (Pfam, Finn 2012), Clusters of Orthologous Groups of

158   proteins (COG, Tatusov *et al.* 2003), and Kyoto Encyclopedia of Genes and Genomes (KEGG,

159   Kanehisa and Goto 2000) by JGI via the IMG database pipeline (Markowitz *et al.* 2012).

160   In addition, 46 of 52 genomes identified by Parks *et al.* (2013) were represented by

161   complete or partial 16S rRNA gene sequences in the NCBI GenBank database (Benson *et al.*

162   2013), spanning all clades of methylators. We used two different approaches to determine

163   methylator relative abundance and community structure. To determine relative abundance, we

164   combined available methylating sequences with generated sequences and re-preformed *de novo*

165   OTU-picking. We then identified OTUs containing known methylator sequences as potential

166   methylators. Because of high *Deltaproteobacteria* abundance, many closely-related methylator

167   sequences may have clustered with non-methylating *Deltaproteobacteria* in this approach. Thus,

168   to examine methylator community structure, we created a database of known methylator

169   sequences and performed closed-reference OTU-picking in QIIME against this database. In

170   addition, a BLAST database was constructed from all *hgcA* and *hgcB* gene sequences available

171   in GenBank. A BLASTX search was conducted against this database to identify taxonomic

172   affiliation of methylators in our samples; however, our query resulted in no matches, likely due

173   to inadequate sequencing depth.

174   *Statistical analysis.*

175   All analyses, unless otherwise noted, were conducted using the *R* software platform.

176   Shapiro-Wilk tests were used to verify normality and assess the appropriateness of parametric vs.

177   non-parametric tests. Multivariate sediment properties (*e.g.*, sediment geochemistry, extracellular

178   enzyme activity, and DNA quantity) were compared across environments at T0 with Hotelling's

179   T-square Test and post hoc Student's *t*-tests. MeHg production was calculated by subtracting T0

180   from T4 MeHg concentrations; values below detection limit were assigned the detection limit as

181   a value for a conservative estimate of change. MeHg production in DOM-amended vs. control

182   microcosms across environment types were compared using ANOVA followed by Tukey HSD

183   post hoc tests. Because of extreme differences in mercury concentrations in vegetated vs.

184   unvegetated sediment (Table 1), paired unequal variance Student's *t*-tests were used to test for

185   within environment (control vs. DOM) differences in net MeHg production. Changes in DOM

186   indices (FI, freshness, HIX) through time (T0-T4) in each sample group were assessed with

187   linear and quadratic regressions. DOM samples with $SUVA_{254}$ >7 were removed due to

188   fluorescence interference from inorganic molecules. Comparisons of DOM indices between data

189   subsets were conducted with ANOVA and post hoc Tukey HSD.

190   Microbial community dissimilarity matrices based on 16S rRNA sequences were

191   constructed using the weighted UniFrac method (Lozupone *et al.* 2011) in QIIME. We

192   preformed analysis using the full community and within the methylating community. To

193   examine the relative abundance of our methylating OTUs, we removed OTUs with less than

194   eight total occurrences (bottom quartile) in our 91 subsamples to limit artifacts from sequencing

195   errors among rare organisms (methylating OTUs were <1% of sequences). Alpha diversity for

196   each sample was assessed using the PD whole tree metric in QIIME. The relative abundance of

197   methylators was compared within each environment at T0 and T4 (DOM vs. controls) using

198   paired unequal variance Student's *t*-tests.

199   Changes in community membership through time (T0-T4) were assessed with ANOSIM

200   in QIIME. Differences in alpha diversity at T0 were assessed using paired unequal variance

201   Student's *t*-tests. Relative abundances of major clades were assessed between vegetated and

202   unvegetated environments at T0 and changes in clades through time (T0-T4) were assessed using

203   non-parametric Kruskal-Wallis tests with FDR-correct *P* values. SIMPER analysis was

204   conducted using the 'vegan package' to identify OTUs associated with community dissimilarity

205   between T0 and T4 in microcosms receiving DOM. Correlations between methylating clades that

206   exhibited significant changes (Kruskal-Wallis, T0-T4), HIX, and MeHg production were

207   assessed at T4 using the Pearson product-momentum correlation coefficient, grouping DOM-

208   amended and control microcosms within each environment in a single analysis to provide

209   sufficient variation.

210   Increases in the frequency of COGs, Pfams, and KEGG pathways at T4 relative to T0

211   were evaluated using binomial tests. Targets more abundant at T4 (FDR-corrected $P < 0.01$)

212   were examined for correlations with HIX and MeHg production at T4 with the Pearson product-

213   momentum correlation coefficient.

214   **Results.**

215   *Ambient geochemistry and microbiology.*

216   Physicochemical and biological properties of vegetated and unvegetated environments

217   significantly differed (Hotelling $P = 0.004$, Table 1). The unvegetated environment was

218   extremely oligotrophic, with low concentrations of sediment C and N, and both vegetated and

219   unvegetated environments appeared to be N-limited (C:N 16.43 and 20.06). DNA concentration,

220   enzyme activities, and mercury concentrations were an order of magnitude higher within the

221   vegetated environment (Table 1).

222   Microbial community structure was significantly different between the two environments

223   (ANOSIM, $P = 0.001$, R= 1.00), though alpha diversity did not differ and major phyla were

224   similar (Table 1). The relative abundance of methylators was higher in the vegetated

225   environment (*t*-test, $P = 0.02$), and the structure of potential methylators within microbial

226   communities also differed between environments (ANOSIM, $P = 0.001$, R = 0.99).

227   *Microbiome response to HgCl$_2$ and DOM addition.*

228   Over the course of the incubation, microcosms with vegetated, high-C sediment produced

229   over ten times more MeHg than unvegetated sediment microcosms, regardless of DOM

230   amendment (ANOVA $P = 0.002$, Tukey HSD, control $P = 0.01$, DOM $P = 0.007$, Figure 1). In

231   addition, mercury methylation was significantly enhanced by DOM addition within the

232   unvegetated nutrient-poor environment with roughly two to four times more production in

233   microcosms receiving DOM as compared to controls (t-test, $P = 0.04$, Figure 1). However, DOM

234   addition did not stimulate significantly more MeHg production than control replicates in the

235   vegetated environment (t-test, $P > 0.05$, Figure 1).

236   Community membership changed through time in vegetated and unvegetated

237   environments amended with DOM (ANOSIM T0-T4, veg.: $P = 0.001$ R $= 0.40$, unveg.: $P =$

238   0.001 R $= 0.43$, Figure S1A and B), but not in controls (veg.: $P = 0.02$, R $= 0.19$, unveg.: $P >$

239   0.05, Figure S1C and D), indicating no substantial effect from high concentrations of added

240   mercury. At T4, communities in unvegetated microcosms amended with DOM were different

241   than controls (ANOSIM, $P = 0.01$, R $= 0.54$), while structure in vegetated sediment microcosms

242   only weakly differed between control and DOM-amended groups ($P = 0.04$, R $= 0.22$). When

243   examining only potential methylators, the relative abundance of methylators was significantly

244   greater in the DOM-amended microcosms versus controls for each environment at T4 (Figure

245   2A, t-test, veg.: $P = 0.03$, unveg.: $P = 0.05$). However, for both environments, there were no

246   significant changes in community membership within methylating clades through time

247   (ANOSIM, T0-T4, $P > 0.05$). This result was not unexpected given our small sample sizes

248   (methylator OTUs contained less than 1% of sequences).

249   Variation in community membership in response to DOM addition was partially

250   generated by an increase in *Clostridia* in both environments (Kruskal-Wallis, veg.: FDR-

251   corrected $P = 0.003$, unveg.: $P = 0.018$, Figure 2B, Table S3) and a decrease in

252   *Deltaproteobacteria* in unvegetated sediment (Kruskal-Wallis, veg.: FDR-corrected $P = 0.36$,

253   unveg.: FDR-corrected $P = 0.015$, Figure 2B). In particular, *Clostridia* abundances increased by

254   3-fold (1.1% to 3.8% of the microbiome) and 10-fold (1.5% to 10.5% of the microbiome),

255   respectively in vegetated and unvegetated environments, driven by increases in nearly all

256   families of *Clostridia*. These shifts were mirrored within our subset of data containing only

257   suspected methylators (Figure 2C), which showed distinct (non-significant) trends for increases

258   in *Clostridia* and decreases in *Deltaproteobacteria* in response to DOM addition in both

259   environments.

260   Changes in the methylating community were more evident at finer taxonomic levels. One

261   family of *Clostridia* (*Peptococcaceae*), sharply increased with DOM addition in unvegetated

262   sediment and displayed a similar trend in vegetated sediment (Kruskal-Wallis, veg.: FDR-

263   corrected $P = 0.18$, unveg.: FDR-corrected $P = 0.04$, Figure 2D). These changes were due to

264   increases in two closely related methylating OTUs (Kruskal-Wallis, *Dehalobacter restrictus*

265   veg.: FDR-corrected $P = 0.24$ (uncorrected $P = 0.04$), and *Syntrophobotulus glycolicus*, unveg.:

266   FDR-corrected $P = 0.006$) grouped in a single genus by our classification system

267   (*Dehalobacter_Syntrophobotulus*, Kruskal-Wallis, veg.: FDR-corrected $P = 0.09$, unveg.: FDR-

268   corrected $P = 0.0027$, Figure S2). Increases in *Clostridia* (*t*-test, FDR-corrected $P = 0.006$),

269   *Peptococcaceae* (*t*-test, FDR-corrected $P = 0.018$), *Dehalobacter restrictus* (*t*-test, FDR-

270   corrected $P = 0.024$), and *Syntrophobotulus glycolicus* (*t*-test, FDR-corrected $P = 0.042$) as well

271   as a possible trend for decreases in *Deltaproteobacteria* (*t*-test, FDR-corrected $P = 0.18$) were

272   also reflected in metagenomic data (Figure 3D).

273   SIMPER analysis of 16S rRNA genes associated with methylator taxonomy in

274   unvegetated DOM-amended microcosms indicated that two OTUs, in *D. restrictus* (increase) and

275   in *Geobacter* (decrease), significantly contributed to community differences between T0 and T4

276   ($P < 0.05$, Table S1). This was reflective of broader changes in the full community, in which

277   22.9% of 175 SIMPER-identified OTUs belonged to *Clostridia* (increased from avg. 0.78

278   OTUs/sample to avg. 17.20 OTUs/sample, Table S3) while 8% belonged to *Deltaproteobacteria*

279   (decreased from avg. 8.5 OTUs/sample to 7.4 OTUs/sample, Table S2).

280   In total, 7,150 KEGG pathways, 84 COGs, and 79 Pfams were significantly more

281   abundant at T4 relative to T0 in unvegetated DOM-amended microcosms (Figure 3A-C). All

282   classfication systems revealed metabolic shifts towards glycosyltranseferases, among other

283   pathways involved in DOM oxidation and in iron and nitrate reduction.

284   *Changes in DOM chemistry.*

285   Details of DOM quantity and quality changes are presented in the Supplemental Material

286   and regression statistics are presented in Table 2. Control microcosms for both environments

287   displayed increasing NPOC concentrations (Figure S3A), while total fluorescence (Figure S3C)

288   and the ratio of fluorescence to NPOC concentration (Figure S3E) displayed non-significant

289   trends or decreased. Within DOM-amended microcosms, vegetated microcosms displayed a

290   decrease in NPOC concentration (Figure S3B), while unvegetated microcosms had stable NPOC

291   content (Figure S3B). Total fluorescence remained stable in both environments (Figure S3D).

292   The ratio of fluorescence-to-NPOC was variable through time and did not statistically change in

293   either environment (Figure S3F).

294   DOM fluorescence indices displayed notable changes through time. In the vegetated

295   environment, FI remained stable at a low value in DOM-amended microcosms, indicating plant-

296   derived DOM, and rose in controls indicating greater relative contribution of microbial vs.

297   abiotic processing (Figure 4A and B). In contrast, in the vegetated environment, HIX increased

298   in both control and DOM-amended microcosms indicating processing of more labile vs.

299   recalcitrant DOM (Figure 4C and D). This increase in HIX corresponded with decrease in

300   freshness (Figure 4E and F), further supporting our interpretation. In the unvegetated

301   environment, DOM-amended microcosms (but not controls) increased in FI (Figure 4A and B)

302   denoting progressively microbial DOM sources. There was no change in HIX (Figure 4C and D)

303   suggesting equal processing of labile vs. recalcitrant DOM. Freshness varied non-linearly in

304   DOM-amended but not control microcosms (Figure 4E and F).

305   Across environment types, HIX was significantly higher in vegetated microcosms

306   (ANOVA $P < 0.0001$, Tukey HSD, DOM-amended: $P < 0.0001$, control: $P = 0.004$). FI and

307   freshness were higher in unvegetated DOM-amended microcosms than in vegetated DOM-

308   amended microcosms (Tukey HSD, FI: $P = 0.003$, freshness: $P = 0.03$) but did not differ across

309   control microcosms (Tukey HSD, FI: $P = 0.89$, freshness: $P = 0.40$).

310   *Correlation of microbiome, DOM characteristics, and MeHg production.*

311   Given the apparent shift in community structure towards *Clostridia,* and

312   (chemoorganotrophic) *Peptococcaceae* in particular, we examined correlations of this family

313   with the proportion of complex organic matter (HIX) and MeHg production within each

314   environment. We focused on HIX because this index changed consistently and reflected portions

315   of recalcitrant carbon substrate pools utilized by the organisms we identified. Because we only

316   calculated MeHg production at the conclusion of the incubation, we analyzed these correlations

317   at T4 and grouped DOM-amended and control replicates within each environment to provide

318   sufficient variation and sample size. *Peptococcaceae* was negatively correlated with HIX and

319   positively correlated with MeHg production in unvegetated microcosms (Pearson's r ($n = 6$),

320   HIX: $P = 0.001$, $r = -0.96$, MeHg: $P = 0.03$, $r = 0.81$). *Peptococcaceae* abundance in vegetated

321   microcosms did not correlate with HIX ($P = 0.20$) or MeHg production ($P = 0.45$).

322   Finally, despite low statistical power ($n = 3$), we observed marginally significant trends

323   ($P < 0.10$) between key metabolic pathways and HIX (Table 3). In particular, COGs classified

324   as: Glycosyltransferase, Glycosyltransferases involved in cell wall biogenesis,

325   Glycosyltransferases - probably involved in cell wall biogenesis, and

326   Beta-galactosidase/beta-glucuronidase; and Pfams classified as: Glycosyl transferase family 2,

327   Radical SAM superfamily, and SusD family displayed significant correlations with HIX at the P

328   < 0.10 level. Only Pfam PF00593, TonB dependent receptor, correlated with MeHg production

329   ($P < 0.001$, $r = -1.00$, Table 2).

330
331   **Discussion.**

332   *Mercury methylation across environments.*

333   Geochemical and microbial characteristics varied across environments, resulting in

334   differential patterns of net MeHg production. Within the vegetated high-C environment, DOM

335   and HgCl$_2$ addition did not influence the sediment microbiome or net MeHg production to the

336   same extent as within the unvegetated environment (Figure 1, Figure S1). Given high ratios of

337   C:N, high OC content, and low NO$_3^-$ concentrations in our vegetated sediment (Table 1), N-

338   limitation may have mitigated net MeHg production in vegetated environments relative to the

339   unvegetated environment (Taylor and Townsend 2010), which had substantially lower

340   concentrations of all measured C and nutrient concentrations. Both ambient MeHg levels and net

341   MeHg production were an order of magnitude higher in the vegetated environment, supporting

342   other findings that plant-microbe interactions inherently facilitates MeHg production (Roy *et al.*

343   2009, Windham-Myers *et al.* 2014, Windham‑Myers *et al.* 2009). Indeed, the vegetated

344   environment displayed higher ambient DNA concentration, enzyme activities, and methylator

345   abundance, underlying a higher *in situ* rate of biological activity.

346   By contrast, the oligotrophic unvegetated environment experienced a dramatic increase in

347   MeHg (Figure 1) in response to DOM and $HgCl_2$ addition that correlated with changes in the

348   sediment microbiome (Figure 2 and 3, Figure S1). Carbon limitation has been widely

349   demonstrated as a constraint on microbial activity (Bradley *et al.* 1992, Brooks *et al.* 2005, Wett

350   and Rauch 2003); thus, DOM addition may bolster MeHg production in C-limited ecosystem

351   from resultant increases in microbial activity. In our system, net MeHg production in the

352   unvegetated environment was possibly also constrained by low *in situ* rates of microbial activity

353   and by low N concentration, and net MeHg production in response to DOM stimulus never

354   increased to vegetated levels. Importantly, DOM enhanced the relative abundance of putative

355   methylators within the microbiome in both environments, indicating that mercury methylation

356   rates may be dually influenced by the sediment microbiome and by organic matter (Aiken *et al.*

357   2011, Hsu-Kim *et al.* 2013).

358   *Microbiome response to $HgCl_2$ and DOM addition.*

359   Our results bolster support for recent work demonstrating preferential organic

360   degradation by *Clostridial* fermentation over organic matter processing by *Deltaproteobacteria*

361   (Reimers *et al.* 2013) and provide support for the involvement of this clade in MeHg production.

362   Within both environments, DOM amendment altered the sediment microbiome, with structural

363   shifts denoting an increase in *Clostridia* and decrease in *Deltaproteobacteria*. Unvegetated

364   microcosms displayed greater changes in these clades, supporting a greater role for

365   environmental filtering by DOM within oligotrophic environments (Barberán *et al.* 2012, Stegen

366   *et al.* 2012). *Clostridia* are obligate anaerobes with the ability to produce labile carbon

367   compounds via fermentation of recalcitrant organic matter (Reimers *et al.* 2013, Ueno *et al.*

368   2016). Recent work has shown organic carbon degradation via *Clostridial* fermentation to

369   operate at comparable rates to more energetically favorable carbon processing pathways

370   (Reimers *et al.* 2013). Moreover, organic acids (*e.g.*, lactate and acetate) produced through these

371   pathways can be subsequently utilized as a carbon source by sulfate- and iron- reducing

372   *Deltaproteobacteria* (Guerrero-Barajas *et al.* 2011, Reimers *et al.* 2013, Zhao *et al.* 2008).

373   Importantly, microbiome changes were mirrored when examining putative methylators

374   independently. Specifically, *Deltaproteobacteria* and *Clostridia*, respectively, were the most

375   abundant methylating organisms at the end of the incubation in all experimental groups except

376   vegetated controls.

377   In unvegetated sediments, although no methylating pathways were identified,

378   metagenomic analyses indicated an increase in carbon, and secondarily, iron metabolisms,

379   supporting a role for microbial carbon and iron cycling in mercury methylation (Gilmour *et al.*

380   2013, Hamelin *et al.* 2011, Kerin *et al.* 2006, Podar *et al.* 2015). Carbon metabolisms were the

381   primary KEGG category increasing in abundance within metagenomes (Figure 3A), and several

382   COG pathways and Pfams indicated a possible metabolic shift favoring glycosyltransferases that

383   convert starches, sugars, and nitroaromatics into a wide range of compounds (Bowles *et al.* 2005,

384   Ramli *et al.* 2015, Figure 3B and C). Further, metagenomic increases in Beta-galactosidase/beta-

385   glucoronidase (lactose to galactose/glucose, Martini *et al.* 1987), sugar phosphate

386   isomerase/epimerases (sugar metabolism, Yeom *et al.* 2013), and lactoylglutathione lyase

387   (detoxification for methyglyoxal fermentation byproduct, Inoue and Kimura 1995) and the SusD

388   family (glycan binding, Martens *et al.* 2009) provide additional evidence increases in

389 fermentation processes in response to DOM addition. Increases in TonB dependent receptors

390 (Moeck and Coulton 1998), amidohydrolase (Seibert and Raushel 2005), and NRAMP (Cellier *et*

391 *al.* 1995) suggest a secondary importance of iron processing and/or transport of large organic

392 compounds across cellular membranes. Finally, our results provide a possible genetic mechanism

393 connecting iron, sulfur, carbon, and mercury cycling, as the radical SAM superfamily, which

394 facilitates methyl transfers via the use of a [4Fe-S]+ cluster (Booker and Grove 2010), increased

395 in concert with net MeHg production. In total, the metabolic potential of the sediment

396 microbiome indicates changes in carbon and iron metabolisms within microcosms experiencing

397 higher net MeHg production in response to DOM addition, supporting past work that suggests a

398 linkage between mercury methylation and these factors (Gilmour *et al.* 2013, Hamelin *et al.*

399 2011, Hsu-Kim *et al.* 2013, Kerin *et al.* 2006, Podar *et al.* 2015).

400   Lastly, at high taxonomic resolution in both environments, DOM addition increased the

401 proportion of methylating organisms classified as *Peptococcaceae* within *Clostridia*, despite

402 drastic differences in sediment chemistry (Figure 2D). Specifically, the two OTUs displaying the

403 greatest change are thought to generate energy via organohalide respiration (*D. restrictus*) and

404 fermentative oxidation of organic matter (*S. glycolicus*, also capable of syntrophy, Han *et al.*

405 2011, Stackebrandt 2014). The relative abundance of *Peptococcaceae* was positively correlated

406 with MeHg production in the unvegetated environment, and other methylating organisms did not

407 increase in abundance, as would be expected if the activity of these organisms was enhanced by

408 DOM addition.

409 *Associations between microbiology, DOM processing, and net MeHg production.*

410   The processing of proportionally more labile organic matter would be expected to result

411 in decreases in DOM freshness and increases in HIX. However, our results suggest substantial

412   contributions of recalcitrant organic matter processing within the unvegetated environment (but

413   not the vegetated environment which followed expectations). In unvegetated microcosms

414   (controls and DOM-amended), HIX did not rise through time indicating relcatritant matter

415   processing (Figure 4C and D). Further, DOM-amended unvegetated microcosms, which

416   experienced pronounced changes in the sediment microbiome and high MeHg production, HIX

417   was significantly lower than in all other experimental groups (ANOVA, $P < 0.0001$, all Tukey

418   HSD $P < 0.0001$). While most microorganisms preferentially degrade labile C sources, the

419   degradation of recalcitrant organic matter can contribute substantially to aquatic carbon cycling

420   (Mcleod *et al.* 2011). DOM-amended unvegetated microcosms also exhibited large increases in

421   microbially-derived DOM (FI) through time, demonstrating a noticeable contribution of

422   microbial activity to the DOM pool (Figure 4A).

423   The abundance of methylating *Peptococcaceae* in unvegetated microcosms negatively

424   correlated with HIX, denoting an apparent contribution of these members or co-occuring

425   community members to DOM processing, but the mechanisms behind these shifts remain

426   unclear. Metabolism of recalcitrant organic matter by fermenting organisms may influence

427   mercury methylation via direct and indirect mechanisms. Members of *Clostridia* can generate

428   MeHg themselves, and *Clostridial* degradation of recalcitrant organic matter can also produce

429   bioavailable carbon substrates for sulfate- and iron- reducing organisms that produce MeHg

430   (Reimers *et al.* 2013).

431   Changes in metagenomes in responses to DOM and inorganic mercury addition elucidate

432   metabolic pathways that may be involved in recalcitrant organic matter processing and MeHg

433   production. For example, both COG and Pfam glycosyltransferases were negatively correlated

434   with HIX, suggesting a role for starch, sugar, and nitroaromatic fermentation in response to

435   DOM loading. As well, a negative correlation between HIX, and the radical SAM superfamily

436   provides a possible mechanistic linkage between methyl transfers and recalcitrant organic matter

437   processing. Conversely, Beta-galactosidase/beta-glucuronidase, and the SusD family were

438   positively correlated with HIX, indicating a co-association with labile C processing rather than

439   recalcitrant organic matter. Only one abundant Pfam – a TonB dependent receptor, signaling

440   enzyme that may be involved in iron cycling (Moeck and Coulton 1998) – and no COGs was

441   correlated with MeHg production. Although our results do not provide a direct linkage between

442   metabolic pathways and mercury methylation, it is notable that no pathways associations involve

443   sulfate-reducing or methanogenic methylators.

444   *Conclusions.*

445   Microbiome shifts towards fermentation pathways, increases in chemoorganotrophic

446   *Clostridia,* degradation of recalcitrant organic matter, and increases in MeHg within oligotrophic

447   environments begin to elucidate the microbial ecology of mercury methylation. While we

448   observed evidence for changes in the microbiome of both high-C and nutrient-poor sediment, the

449   more oligotrophic environment showed greater responses in the sediment microbiome and in

450   mercury methylation to the addition of DOM, an important insight given increasing risks of

451   anthropogenic eutrophication. Importantly, our results provide evidence for organisms not

452   historically considered in MeHg production and suggest future work into the environmental

453   relevance of these organisms in mercury methylation. *Clostridia* thrive in a variety of anoxic

454   environments from wastewater effluent (Wang *et al.* 2003) to the human gut (Mahowald *et al.*

455   2009), and our work supports the potential for mercury methylation across a broad range of

456   ecological niches (Gilmour *et al.* 2013, Podar *et al.* 2015). Taken together, our research provides

457   new insights into microorganisms impacting MeHg production in natural settings and

458   emphasizes the importance of exploring microbial physiology not typically associated with

459   methylating organisms in enhancing mercury toxicity.

460

470

471

472

References.

Aiken GR, Hsu-Kim H, Ryan JN (2011). Influence of dissolved organic matter on the environmental fate of metals, nanoparticles, and colloids. *Environmental science & technology* **45:** 3196-3201.

Bae H-S, Dierberg FE, Ogram A (2014). Syntrophs Dominate Sequences Associated with the Mercury Methylation-Related Gene hgcA in the Water Conservation Areas of the Florida Everglades. *Applied and environmental microbiology* **80:** 6517-6526.

Barberán A, Bates ST, Casamayor EO, Fierer N (2012). Using network analysis to explore co-occurrence patterns in soil microbial communities. *The ISME journal* **6:** 343-351.

Benoit J, Gilmour C, Heyes A, Mason R, Miller C (2003). Geochemical and biological controls over methylmercury production and degradation in aquatic ecosystems. *ACS symposium series* **835:** 262-297.

Benson DA, Cavanaugh M, Clark K, Karsch-Mizrachi I, Lipman DJ, Ostell J *et al* (2013). GenBank. *Nucleic acids research* **41:** D36-D42.

Booker SJ, Grove TL (2010). Mechanistic and functional versatility of radical SAM enzymes. *F1000 Biol Rep* **2:** 52.

Bowles D, Isayenkova J, Lim E-K, Poppenberger B (2005). Glycosyltransferases: managers of small molecules. *Current opinion in plant biology* **8:** 254-263.

Bradley P, Fernandez Jr M, Chapelle F (1992). Carbon limitation of denitrification rates in an anaerobic groundwater system. *Environmental science & technology* **26:** 2377-2381.

Branfireun BA, Roulet NT, Kelly C, Rudd JW (1999). In situ sulphate stimulation of mercury methylation in a boreal peatland: Toward a link between acid rain and methylmercury contamination in remote environments. *Global Biogeochemical Cycles* **13:** 743-750.

Brooks PD, McKnight D, Elder K (2005). Carbon limitation of soil respiration under winter snowpacks: potential feedbacks between growing season and winter carbon fluxes. *Global Change Biology* **11:** 231-238.

Caporaso JG, Kuczynski J, Stombaugh J, Bittinger K, Bushman FD, Costello EK *et al* (2010). QIIME allows analysis of high-throughput community sequencing data. *Nature methods* **7:** 335-336.

Caporaso JG, Lauber CL, Walters WA, Berg-Lyons D, Huntley J, Fierer N *et al* (2012). Ultra-high-throughput microbial community analysis on the Illumina HiSeq and MiSeq platforms. *The ISME journal* **6:** 1621-1624.

517 Cellier M, Prive G, Belouchi A, Kwan T, Rodrigues V, Chia W *et al* (1995). Nramp defines a
518 family of membrane proteins. *Proceedings of the National Academy of Sciences* **92:** 10089-
519 10093.

521 Compeau G, Bartha R (1984). Methylation and demethylation of mercury under controlled
522 redox, pH and salinity conditions. *Applied and Environmental Microbiology* **48:** 1203-1207.

524 Compeau G, Bartha R (1985). Sulfate-reducing bacteria: principal methylators of mercury in
525 anoxic estuarine sediment. *Applied and environmental microbiology* **50:** 498-502.

527 Docherty KM, Young KC, Maurice PA, Bridgham SD (2006). Dissolved organic matter
528 concentration and quality influences upon structure and function of freshwater microbial
529 communities. *Microbial Ecology* **52:** 378-388.

531 Drexel RT, Haitzer M, Ryan JN, Aiken GR, Nagy KL (2002). Mercury (II) sorption to two
532 Florida Everglades peats: Evidence for strong and weak binding and competition by dissolved
533 organic matter released from the peat. *Environmental science & technology* **36:** 4058-4064.

535 Edgar RC (2013). UPARSE: highly accurate OTU sequences from microbial amplicon reads.
536 *Nature methods* **10:** 996-998.

538 Fellman JB, Hood E, Spencer RG (2010). Fluorescence spectroscopy opens new windows into
539 dissolved organic matter dynamics in freshwater ecosystems: A review. *Limnology and
540 Oceanography* **55:** 2452-2462.

542 Finn RD (2012). Pfam: the protein families database. *Encyclopedia of Genetics, Genomics,
543 Proteomics and Bioinformatics*.

545 Forsström L, Roiha T, Rautio M (2013). Responses of microbial food web to increased
546 allochthonous DOM in an oligotrophic subarctic lake. *Aquatic microbial ecology* **68:** 171-184.

548 Gabor RS, Baker A, McKnight DM, Miller MP (2014a). Fluorescence Indices and Their
549 Interpretation. *Aquatic Organic Matter Fluorescence***:** 303.

551 Gabor RS, Eilers K, McKnight DM, Fierer N, Anderson SP (2014b). From the litter layer to the
552 saprolite: Chemical changes in water-soluble soil organic matter and their correlation to
553 microbial community composition. *Soil Biology and Biochemistry* **68:** 166-176.

555 Gilmour CC, Podar M, Bullock AL, Graham AM, Brown SD, Somenahally AC *et al* (2013).
556 Mercury methylation by novel microorganisms from new environments. *Environmental science
557 & technology* **47:** 11810-11820.

559 Graham AM, Aiken GR, Gilmour CC (2013). Effect of dissolved organic matter source and
560 character on microbial Hg methylation in Hg–S–DOM solutions. *Environmental science &
561 technology* **47:** 5746-5754.

563 Graham EB, Knelman JE, Schindlbacher A, Siciliano S, Breulmann M, Yannarell A *et al* (2016).
564 Microbes as engines of ecosystem function: When does community structure enhance
565 predictions of ecosystem processes? *Frontiers in microbiology* **7**.
566
567 Guerrero-Barajas C, Garibay-Orijel C, Rosas-Rocha LE (2011). Sulfate reduction and
568 trichloroethylene biodegradation by a marine microbial community from hydrothermal vents
569 sediments. *International Biodeterioration & Biodegradation* **65:** 116-123.
570
571 Haitzer M, Aiken GR, Ryan JN (2002). Binding of mercury (II) to dissolved organic matter: the
572 role of the mercury-to-DOM concentration ratio. *Environmental Science & Technology* **36:**
573 3564-3570.
574
575 Hamelin S, Amyot M, Barkay T, Wang Y, Planas D (2011). Methanogens: principal methylators
576 of mercury in lake periphyton. *Environmental science & technology* **45:** 7693-7700.
577
578 Hamelin S, Planas D, Amyot M (2015). Mercury methylation and demethylation by periphyton
579 biofilms and their host in a fluvial wetland of the St. Lawrence River (QC, Canada). *Science of*
580 *the Total Environment* **512:** 464-471.
581
582 Han C, Mwirichia R, Chertkov O, Held B, Lapidus A, Nolan M *et al* (2011). Complete genome
583 sequence of Syntrophobotulus glycolicus type strain (FlGlyRT). *Standards in genomic sciences*
584 **4:** 371.
585
586 Harmon S, King J, Gladden J, Chandler GT, Newman L (2005). Mercury body burdens in
587 Gambusia holbrooki and Erimyzon sucetta in a wetland mesocosm amended with sulfate.
588 *Chemosphere* **59:** 227-233.
589
590 Harris-Hellal J, Vallaeys T, Garnier-Zarli E, Bousserrhine N (2009). Effects of mercury on soil
591 microbial communities in tropical soils of French Guyana. *Applied Soil Ecology* **41:** 59-68.
592
593 Hintelmann H, Keppel‐Jones K, Evans RD (2000). Constants of mercury methylation and
594 demethylation rates in sediments and comparison of tracer and ambient mercury availability.
595 *Environmental toxicology and chemistry* **19:** 2204-2211.
596
597 Hsu-Kim H, Kucharzyk KH, Zhang T, Deshusses MA (2013). Mechanisms regulating mercury
598 bioavailability for methylating microorganisms in the aquatic environment: a critical review.
599 *Environmental science & technology* **47:** 2441-2456.
600
601 Inoue Y, Kimura A (1995). Methylglyoxal and regulation of its metabolism in microorganisms.
602 *Advances in microbial physiology* **37:** 177.
603
604 Jeremiason JD, Engstrom DR, Swain EB, Nater EA, Johnson BM, Almendinger JE *et al* (2006).
605 Sulfate addition increases methylmercury production in an experimental wetland. *Environmental*
606 *science & technology* **40:** 3800-3806.
607

608 Kanehisa M, Goto S (2000). KEGG: kyoto encyclopedia of genes and genomes. *Nucleic acids*
609 *research* **28:** 27-30.
610
611 Kerin EJ, Gilmour C, Roden E, Suzuki M, Coates J, Mason R (2006). Mercury methylation by
612 dissimilatory iron-reducing bacteria. *Applied and environmental microbiology* **72:** 7919-7921.
613
614 King JK, Kostka JE, Frischer ME, Saunders FM (2000). Sulfate-reducing bacteria methylate
615 mercury at variable rates in pure culture and in marine sediments. *Applied and Environmental*
616 *Microbiology* **66:** 2430-2437.
617
618 Knelman JE, Legg TM, O'Neill SP, Washenberger CL, González A, Cleveland CC *et al* (2012).
619 Bacterial community structure and function change in association with colonizer plants during
620 early primary succession in a glacier forefield. *Soil Biology and Biochemistry* **46:** 172-180.
621
622 Lambertsson L, Nilsson M (2006). Organic material: the primary control on mercury methylation
623 and ambient methyl mercury concentrations in estuarine sediments. *Environmental science &*
624 *technology* **40:** 1822-1829.
625
626 Liu Y-R, Yu R-Q, Zheng Y-M, He J-Z (2014a). Analysis of the Microbial Community Structure
627 by Monitoring an Hg Methylation Gene (hgcA) in Paddy Soils along an Hg Gradient. *Applied*
628 *and environmental microbiology* **80:** 2874-2879.
629
630 Liu Y-R, Zheng Y-M, Zhang L-M, He J-Z (2014b). Linkage between community diversity of
631 sulfate-reducing microorganisms and methylmercury concentration in paddy soil. *Environmental*
632 *Science and Pollution Research* **21:** 1339-1348.
633
634 Lozupone C, Lladser ME, Knights D, Stombaugh J, Knight R (2011). UniFrac: an effective
635 distance metric for microbial community comparison. *The ISME journal* **5:** 169.
636
637 Lu X, Liu Y, Johs A, Zhao L, Wang T, Yang Z *et al* (2016). Anaerobic mercury methylation and
638 demethylation by Geobacter bemidjiensis Bem. *Environmental science & technology* **50:** 4366-
639 4373.
640
641 Mahowald MA, Rey FE, Seedorf H, Turnbaugh PJ, Fulton RS, Wollam A *et al* (2009).
642 Characterizing a model human gut microbiota composed of members of its two dominant
643 bacterial phyla. *Proceedings of the National Academy of Sciences* **106:** 5859-5864.
644
645 Markowitz VM, Chen I-MA, Palaniappan K, Chu K, Szeto E, Grechkin Y *et al* (2012). IMG: the
646 integrated microbial genomes database and comparative analysis system. *Nucleic acids research*
647 **40:** D115-D122.
648
649 Martens EC, Koropatkin NM, Smith TJ, Gordon JI (2009). Complex glycan catabolism by the
650 human gut microbiota: the Bacteroidetes Sus-like paradigm. *Journal of Biological Chemistry*
651 **284:** 24673-24677.
652

653 Martini MC, Bollweg GL, Levitt MD, Savaiano DA (1987). Lactose digestion by yogurt beta-
654 galactosidase: influence of pH and microbial cell integrity. *The American journal of clinical*
655 *nutrition* **45:** 432-436.
656
657 Mcleod E, Chmura GL, Bouillon S, Salm R, Björk M, Duarte CM *et al* (2011). A blueprint for
658 blue carbon: toward an improved understanding of the role of vegetated coastal habitats in
659 sequestering CO2. *Frontiers in Ecology and the Environment* **9:** 552-560.
660
661 Moeck GS, Coulton JW (1998). TonB‐dependent iron acquisition: Mechanisms of siderophore
662 ‐mediated active transport. *Molecular microbiology* **28:** 675-681.
663
664 Morel FM, Kraepiel AM, Amyot M (1998). The chemical cycle and bioaccumulation of
665 mercury. *Annual review of ecology and systematics***:** 543-566.
666
667 Parks JM, Johs A, Podar M, Bridou R, Hurt RA, Smith SD *et al* (2013). The genetic basis for
668 bacterial mercury methylation. *Science* **339:** 1332-1335.
669
670 Pernthaler J (2013). Freshwater microbial communities. *The Prokaryotes*. Springer. pp 97-112.
671
672 Podar M, Gilmour CC, Brandt CC, Soren A, Brown SD, Crable BR *et al* (2015). Global
673 prevalence and distribution of genes and microorganisms involved in mercury methylation.
674 *Science advances* **1:** e1500675.
675
676 Poulain AJ, Orihel DM, Amyot M, Paterson MJ, Hintelmann H, Southworth GR (2006).
677 Relationship between the loading rate of inorganic mercury to aquatic ecosystems and dissolved
678 gaseous mercury production and evasion. *Chemosphere* **65:** 2199-2207.
679
680 Poulain AJ, Barkay T (2013). Cracking the mercury methylation code. *Science* **339:** 1280-1281.
681
682 Ramli N, Abd-Aziz S, Hassan MA, Alitheen N, Kamaruddin K (2015). Potential cyclodextrin
683 glycosyltransferase producer from locally isolated bacteria. *African Journal of Biotechnology* **9:**
684 7317-7321.
685
686 Ravichandran M (2004). Interactions between mercury and dissolved organic matter—a review.
687 *Chemosphere* **55:** 319-331.
688
689 Reimers CE, Alleau Y, Bauer JE, Delaney J, Girguis PR, Schrader PS *et al* (2013). Redox effects
690 on the microbial degradation of refractory organic matter in marine sediments. *Geochimica et*
691 *Cosmochimica Acta* **121:** 582-598.
692
693 Roy V, Amyot M, Carignan R (2009). Beaver ponds increase methylmercury concentrations in
694 Canadian shield streams along vegetation and pond-age gradients. *Environmental science &*
695 *technology* **43:** 5605-5611.
696

697 Ruggiero P, Terzano R, Spagnuolo M, Cavalca L, Colombo M, Andreoni V *et al* (2011). Hg
698 bioavailability and impact on bacterial communities in a long-term polluted soil. *Journal of*
699 *Environmental Monitoring* **13:** 145-156.

701 Seibert CM, Raushel FM (2005). Structural and catalytic diversity within the amidohydrolase
702 superfamily. *Biochemistry* **44:** 6383-6391.

704 Si Y, Zou Y, Liu X, Si X, Mao J (2015). Mercury methylation coupled to iron reduction by
705 dissimilatory iron-reducing bacteria. *Chemosphere* **122:** 206-212.

707 Smith SD, Bridou R, Johs A, Parks JM, Elias DA, Hurt RA *et al* (2015). Site-directed
708 mutagenesis of HgcA and HgcB reveals amino acid residues important for mercury methylation.
709 *Applied and environmental microbiology* **81:** 3205-3217.

711 Stackebrandt E (2014). The Emended Family Peptococcaceae and Description of the Families
712 Desulfitobacteriaceae, Desulfotomaculaceae, and Thermincolaceae. *The Prokaryotes*. Springer.
713 pp 285-290.

715 Stegen JC, Lin X, Konopka AE, Fredrickson JK (2012). Stochastic and deterministic assembly
716 processes in subsurface microbial communities. *The ISME journal* **6:** 1653-1664.

718 Tatusov RL, Fedorova ND, Jackson JD, Jacobs AR, Kiryutin B, Koonin EV *et al* (2003). The
719 COG database: an updated version includes eukaryotes. *BMC bioinformatics* **4:** 1.

721 Taylor PG, Townsend AR (2010). Stoichiometric control of organic carbon–nitrate relationships
722 from soils to the sea. *Nature* **464:** 1178-1181.

724 Ueno A, Shimizu S, Tamamura S, Okuyama H, Naganuma T, Kaneko K (2016). Anaerobic
725 decomposition of humic substances by Clostridium from the deep subsurface. *Scientific reports*
726 **6**.

728 Ullrich SM, Tanton TW, Abdrashitova SA (2001). Mercury in the aquatic environment: a review
729 of factors affecting methylation. *Critical reviews in environmental science and technology* **31:**
730 241-293.

732 Wang C, Chang C, Chu C, Lee D, Chang B-V, Liao C (2003). Producing hydrogen from
733 wastewater sludge by Clostridium bifermentans. *Journal of Biotechnology* **102:** 83-92.

735 Waples JS, Nagy KL, Aiken GR, Ryan JN (2005). Dissolution of cinnabar (HgS) in the presence
736 of natural organic matter. *Geochimica et Cosmochimica Acta* **69:** 1575-1588.

738 Wett B, Rauch W (2003). The role of inorganic carbon limitation in biological nitrogen removal
739 of extremely ammonia concentrated wastewater. *Water Research* **37:** 1100-1110.
740

741 Wetzel RG (1992). Gradient-dominated ecosystems: sources and regulatory functions of
742 dissolved organic matter in freshwater ecosystems. *Dissolved organic matter in lacustrine*
743 *ecosystems*. Springer. pp 181-198.
744
745 Windham-Myers L, Marvin-DiPasquale M, Stricker CA, Agee JL, Kieu LH, Kakouros E (2014).
746 Mercury cycling in agricultural and managed wetlands of California, USA: Experimental
747 evidence of vegetation-driven changes in sediment biogeochemistry and methylmercury
748 production. *Science of the Total Environment* **484:** 300-307.
749
750 Windham‐Myers L, Marvin‐Dipasquale M, Krabbenhoft DP, Agee JL, Cox MH, Heredia‐
751 Middleton P *et al* (2009). Experimental removal of wetland emergent vegetation leads to
752 decreased methylmercury production in surface sediment. *Journal of Geophysical Research:*
753 *Biogeosciences (2005–2012)* **114**.
754
755 Yeom S-J, Kim Y-S, Oh D-K (2013). Development of Novel Sugar Isomerases by Optimization
756 of Active Sites in Phosphosugar Isomerases for Monosaccharides. *Applied and environmental*
757 *microbiology* **79:** 982-988.
758
759 Yu R-Q, Reinfelder JR, Hines ME, Barkay T (2013). Mercury methylation by the methanogen
760 Methanospirillum hungatei. *Applied and environmental microbiology* **79:** 6325-6330.
761
762 Zhao Y, Ren N, Wang A (2008). Contributions of fermentative acidogenic bacteria and sulfate-
763 reducing bacteria to lactate degradation and sulfate reduction. *Chemosphere* **72:** 233-242.
764
765 Zhou Z, Zheng Y, Shen J, Zhang L, Liu Y, He J (2012). Responses of activities, abundances and
766 community structures of soil denitrifiers to short-term mercury stress. *Journal of Environmental*
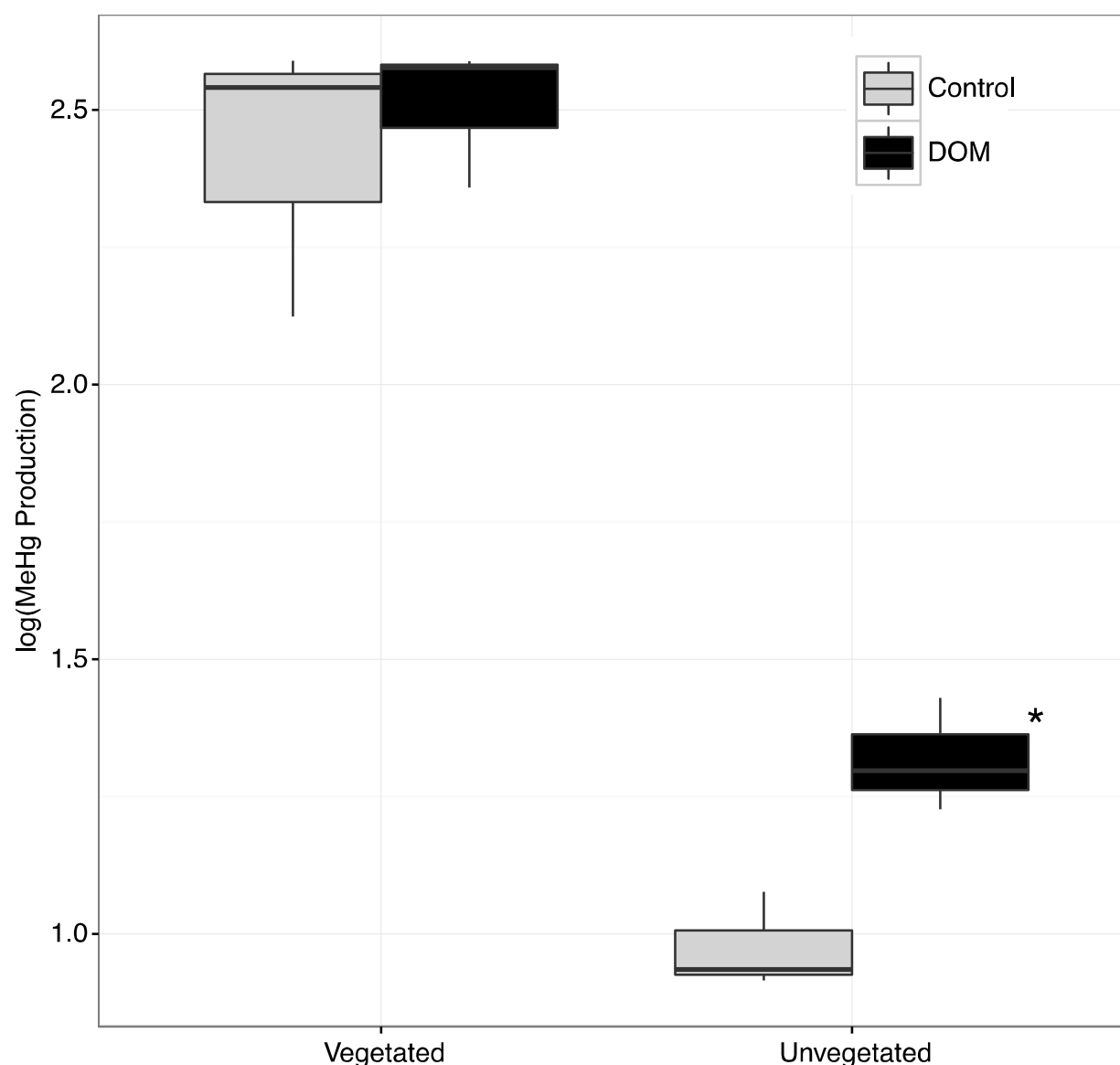767 *Sciences* **24:** 369-375.
768
769

770

771   **Figures.**

772

773
774   **Figure 1.** Boxplots are shown for net MeHg production, with upper and lower hinges
775   representing the values at the 75th and 25th percentiles and whiskers respresenting 1.5 times value
776   at the 75th and 25th percentiles, respectively. DOM did not significantly increase net MeHg
777   production in, vegetated sediment, but induced net MeHg production in unvegetated sediment.
778   Regardless of DOM amendment, vegetated sediment experienced an order of magnitude higher
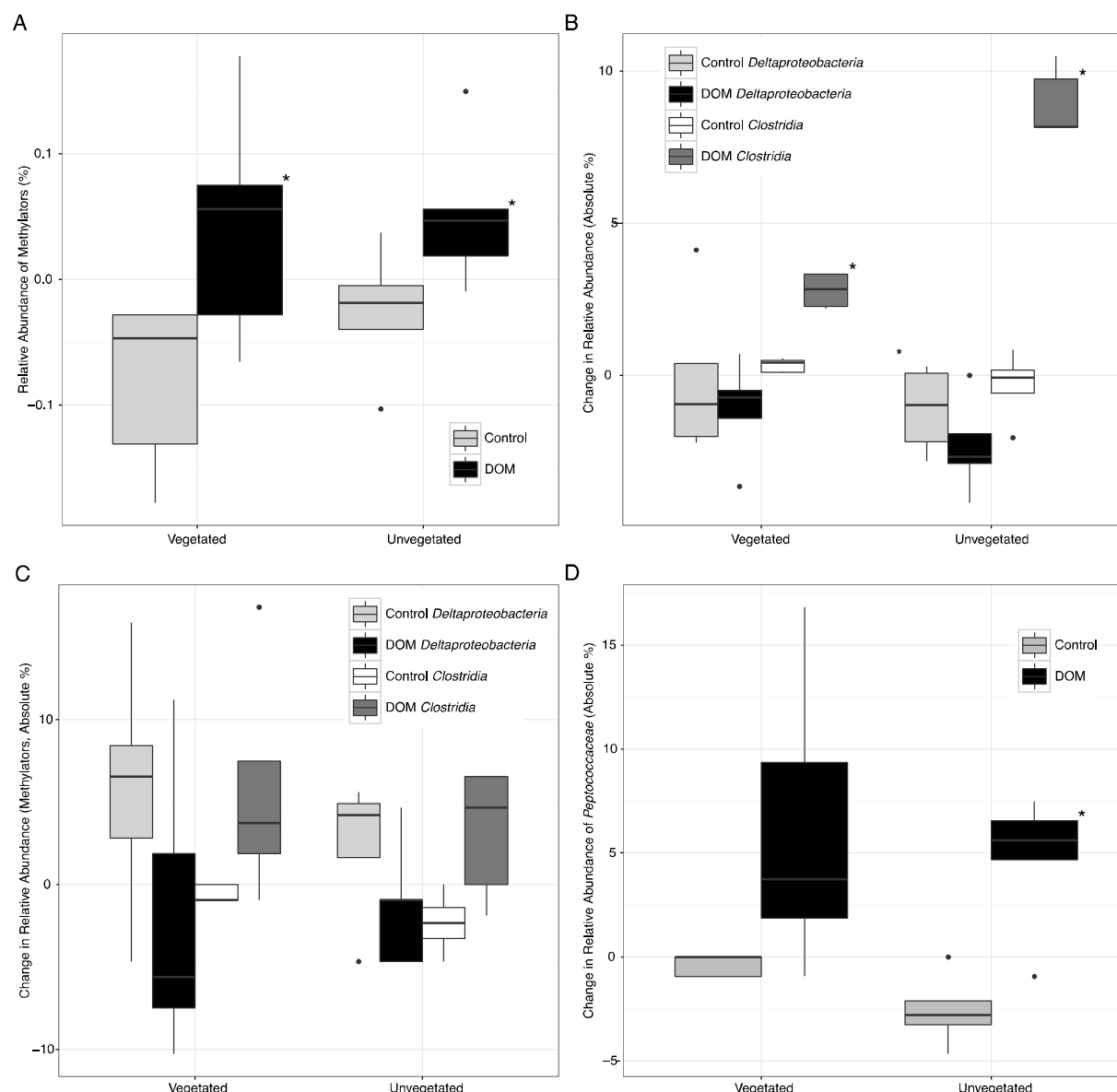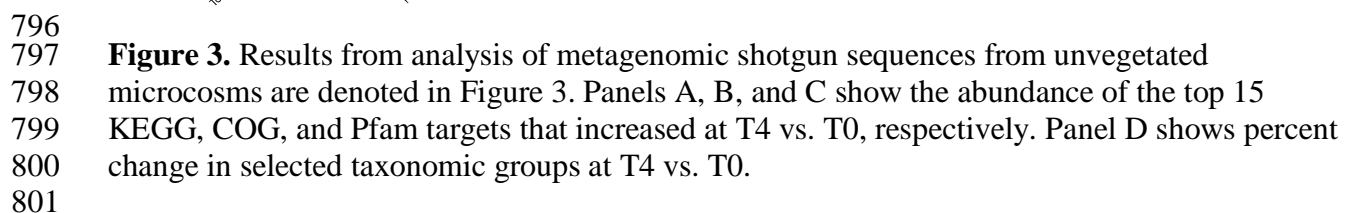779   rates of net mercury methylation.
780
781

Figure 2. Boxplots are shown for selected changes in abundance of methylator abundance (A) and taxonomy (B-D) in response to DOM addition, with upper and lower hinges representing the values at the 75th and 25th percentiles and whiskers respresenting 1.5 times value at the 75th and 25th percentiles, respectively. Outliers are plotted as points. Shading for each bar denote taxonomy and DOM-amended vs. control. Significant relationships ($P < 0.05$) are denoted with an asterisk. (A) The relative abundance of methylating organisms increased in both sediment types in response to DOM addition. (B) The addition of DOM decreased the proportion of *Deltaproteobacteria* and increased the proportion of *Clostridia* in both vegetated and unvegetated sediment, with greater effects in unvegetated sediment. (C) Within potential methylators, *Deltaproteobacteria* decreased and *Clostridia* increased in response to DOM addition, (D) driven by changes within the family *Peptococcaceae*. Abundance data are present in Table S3.
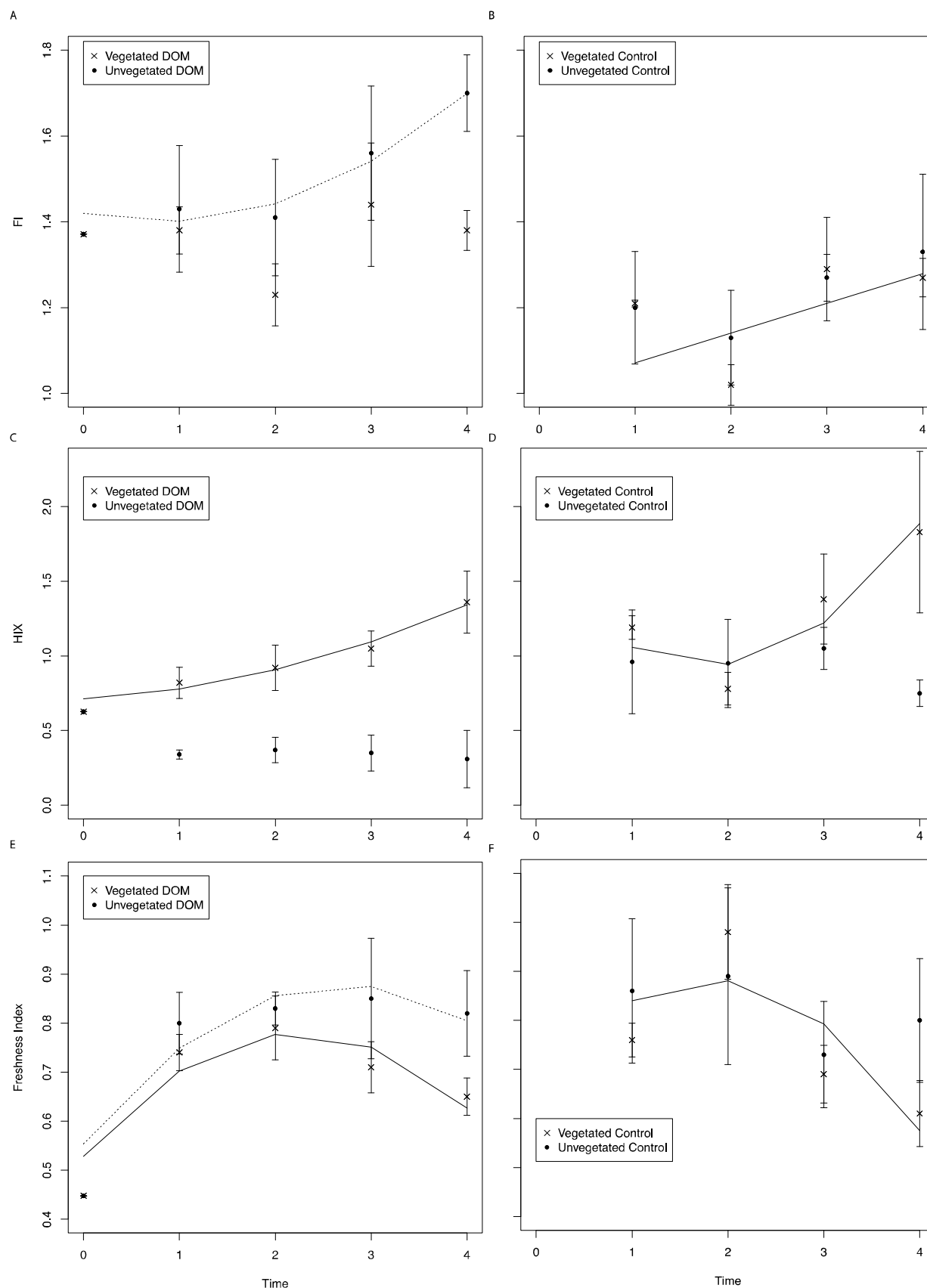
796
Figure 3. Results from analysis of metagenomic shotgun sequences from unvegetated microcosms are denoted in Figure 3. Panels A, B, and C show the abundance of the top 15 KEGG, COG, and Pfam targets that increased at T4 vs. T0, respectively. Panel D shows percent change in selected taxonomic groups at T4 vs. T0.

802

34

803 **Figure 4.** DOM fluorescence indices were assessed through time with linear and quadratic
804 regressions in each environment and microcosm type. Averages for each environment and
805 microcosm type are plotted at T0-T4, with error bars representing the standard deviation. Plots in
806 the first column at DOM-amended microcosms, while plots in the second column are control
807 microcosms. Unvegetated microcsms are depicted as closed circles with dashed lines showing
808 significant regressions; vegetated microcosms are x's with solid lines showing significant
809 regressions. (A) and (B) denote FI, (C) and (D) denote HIX, and (E) and (F) denote freshness.
810
811

812 **Tables.**

813

814 **Table 1.** Mean chemical and biological characteristics of vegetated and unvegetated
815 environments are presented Table 1. Asterisks represent significant differences from post hoc *t*-
816 tests, and standard deviations are presented in parentheses.

817

	Vegetated Environment	Unvegetated Environment
pH*	5.6 (0.09)	5.8 (0.40)
NH4 (mg/L)***	1.49 (0.32)	0.36 (0.14)
TPOC (mg/L)***	1.13 (0.06)	0.09 (0.05)
TDN (mg/L)**	0.06 (0.02)	0.04 (0.01)
percent C***	13.16 (2.20)	1.82 (3.39)
percent N***	0.8 (0.06)	0.1 (0.23)
C:N*	16.43 (1.59)	20.06 (5.36)
DNA concentratin (ng/L)***	28.13 (5.06)	9.31 (3.16)
NAG (nmol/h/g)***	308.94 (181.30)	9.05 (9.29)
BG (nmol/h/g)***	371.22 (81.25)	17.71 (19.29)
PHOS (nmol/h/g)***	393.45 (55.06)	20.69 (17.33)
SMHG (ng/g)**	2.67 (2.18)	0.24 (0.12)
STHG (ng/g)	306.56 (551.07)	3.16 (3.99)
SM/THG	0.02 (0.009)	0.32 (0.45)
Proteobacteria***	0.3 (0.04)	0.43 (0.02)
Chloroflexi***	0.17 (0.01)	0.06 (0.009)
Bacteroidetes	0.11 (0.02)	0.13 (0.03)
Acidobacteria*	0.07 (0.009)	0.08 (0.02)
Nitrospirae***	0.05 (0.009)	0.02 (0.009)
Actinobacteria***	0.03 (0.007)	0.07 (0.01)
Alpha Diversity*	116.73 (6.65)	120.6 (11.33)

*P < 0.10   ** P < 0.05   *** P < 0.01

818
819
820

821 **Table 2.** R^2 values from regression analysis of changes in DOM properties through time are
822 listed in Table 2. Control microcosms were analyzed from T1-T4 and DOM-amended
823 microcosms were analyzed from T0-T4, with characteristics of the applied DOM represented at
824 T0.
825

	NPOC (mg/L)	Total Fluorescence	Fluor:NPOC	FI	HIX	Freshness
Vegetated, Control (T1-T4)	0.39**	0.21*	n.s.	0.22**	0.51***	0.52***
Vegetated, DOM-amended (T0-T4)	0.32***	n.s.	n.s.	n.s.	0.68****	0.57***
Unvegetated, Control (T1-T4)	0.64****	n.s.	0.29**	n.s.	n.s.	n.s.
Unvegetated, DOM-amended (T0-T4)	n.s.	n.s.	n.s.	0.41***	n.s.	0.39***

826 *$P < 0.10$ **$P < 0.05$ ***$P < 0.01$ ****$P < 0.001$
827
828

829 **Table 3.** The Pearson product-momentum correlation coefficient was used to assess relationships
830 of selected COG and Pfam targets with HIX and net MeHg production at T4 ($n = 3$).
831 Relationships are presented in Table 3.

	HIX	MeHg
COG		
Glycosyltransferase	⏤0.98*	0.79
Glycosyltransferases involved in cell wall biogenesis	⏤0.96*	0.76
ABC-type nitrate/sulfonate/bicarbonate transport systems, periplasmic components	-0.85	0.55
FOG: PAS/PAC domain	-0.88	0.60
Predicted metal-dependent hydrolase of the TIM-barrel fold	0.88	0.60
Transcriptional regulator	⏤0.999**	0.88
Outer membrane receptor proteins, mostly Fe transport	-0.79	0.45
HD-GYP domain	⏤0.99**	0.84
Glycosyltransferases, probably involved in cell wall biogenesis	⏤0.96*	0.74
Beta-galactosidase/beta-glucuronidase	0.98*	-0.80
Sugar phosphate isomerases/epimerases	-0.73	0.36
Lactoylglutathione lyase and related lyases	-0.93	0.67
Nitroreductase	⏤0.996**	0.86
Thiamine biosynthesis enzyme ThiH and related uncharacterized enzymes	0.98*	0.80
ABC-type phosphate transport system, periplasmic component	-0.66	0.27
Pfam		
WD40-like Beta Propeller Repeat	⏤0.99**	0.85
Glycosyl transferase family 2	⏤0.97*	0.76
TonB dependent receptor	0.90	⏤0.9999***
Radical SAM superfamily	⏤0.95*	0.75
TonB-dependent Receptor Plug Domain	0.51	-0.83
Amidohydrolase	-0.87	0.57
NMT1/THI5 like	-0.87	0.58
HD domain	⏤0.9997**	0.91
DNA gyrase C-terminal domain, beta-propeller	-0.94	0.70
Protein of unknown function (DUF1501)	-0.46	0.04
RHS Repeat	-0.80	0.46
Doubled CXXCH motif (Paired_CXXCH_1)	⏤0.97*	0.78
Helix-turn-helix	-0.90	0.63
Natural resistance-associated macrophage protein	-0.83	0.51
SusD family	0.99*	-0.82

*$P < 0.10$; **$P < 0.05$

832
833